Copper impurity diffusion in sodium iodide*

Ning-Huat Chan and W. J. Van Sciver
Lehigh University, Bethlehem, Pennsylvania 18015
(Received 28 May 1974; revised manuscript received 28 January 1975)

A thin-layer method was used to study the diffusion of copper in NaI. Final concentration-distance profiles were measured by an optical-absorption method. All plots of $\log_{10}C$ vs z^2 are linear for temperatures below 265°C and above 415°C, and they are curved for temperatures in between. The Arrhenius plot shows two straight segments from which activation energies are calculated to be 1.00 eV for the low-temperature region and 0.65 eV for the high-temperature region. The diffusion coefficient for copper in sodium iodide exceeds the self-diffusion coefficient of sodium in sodium iodide by factors of 10^3–10^4. Thus the diffusion of copper in sodium iodide cannot be explained by the vacancy mechanism, which is the usually accepted one for the alkali halides. The experimental data strongly suggest that above 415°C most of the copper impurity will be interstitial and the diffusion is by a simple interstitial mechanism.

I. INTRODUCTION

From the extensive study of ionic conductivity and self-diffusion measurements, it is generally accepted that Frenkel disorder is the predominant type of point defect in silver halides while Schöttky disorder predominates in alkali halides with the NaCl-type structure. Nevertheless, for cationic impurities in these halides, the nature of the ionic defects is not well understood, especially in the alkali halides. In contrast to the situation in metals, relatively little exploration of the diffusional behavior of impurity ions in the silver and alkali halides has been made. So far, there has been insufficient evidence to justify the existence of interstitial foreign cations in the alkali halides, although copper,[1] gold,[2] cadmium,[3] and manganese[4] have been concluded to occupy interstitial positions as well as lattice sites in the silver halides. From optical-spectroscopy investigation, Nasu (unpublished work) suggests that cobalt occupies interstitial positions in NaCl. However, diffusion of cobalt in[5] NaCl does not indicate this to be the case. Reisfeld and Honigbaum[6] have reported the diffusion of trivalent bismuth ions in KCl. The Arrhenius plot consists of two segments. The authors suggest that in the high-temperature region, bismuth is in its divalent state and diffuses by the usual vacancy mechanism. In the low-temperature region, bismuth diffusion proceeds in the trivalent state and diffuses by an interstitial mechanism. However, the argument which is based solely on the change of slope of the Arrhenius plot and the relatively small activation energy (0.63 eV) can only be a speculation. It is not normally possible to determine whether a break in the Arrhenius plot is due simply to the intrinsic-extrinsic transition and when it is due to a change in mechanism. The value 0.63 eV is not obviously too small for a vacancy mechanism since Zn^{2+} in NaCl,[7] and Ca^{2+} in KCl,[8] have smaller migration energies yet they migrate via a vacancy mechanism.

Since copper,[1] gold,[2] cadmium,[3] and manganese[4] can occupy both interstitial positions and lattice sites in the silver halides, whereas sodium,[9] lithium,[10] strontium,[11] and calcium[12] are likely to occupy lattice sites only, there has been speculation[4,13] on the correlation between outer d-shell electrons and occupied positions, namely, ions with d shells may more readily occupy interstitial positions; this does not seem to follow in the alkali halides. Diffusion study of silver in[14] NaCl and[15] KBr and copper[16] in NaCl and KCl have led to the conclusion that substitutional sites are the occupied positions. However, comparing the diffusion coefficients of copper with that of cationic self-diffusion, one finds that the diffusion coefficients of copper[16] in NaCl and KCl are about three and four orders of magnitude, respectively, larger than the cationic self-diffusion coefficients in the intrinsic temperature region. The ratio of copper diffusion coefficient and cationic self-diffusion coefficient should not exceed about an order of magnitude, if copper and sodium (or potassium) diffuse by the same (vacancy) mechanism in the same host crystal. The rather unusual observed ratios of three and four orders of magnitude indicate that copper is unlikely to migrate via a vacancy mechanism in either NaCl or KCl. But there is no conclusive evidence that copper diffuses interstitially in these crystals.

The investigation which is reported here gives diffusion data of copper in NaI over a temperature range from 190 to 570°C. The data show strong evidence that Frenkel disorder does indeed exist for copper in NaI.

II. EXPERIMENTAL

All NaI samples were obtained from Harshaw Chemical Company. Optical-absorption measurements indicated that these "pure" samples contain $(1.3 \pm 0.1) \times 10^{-7}$ mole fraction of copper. From the conductivity measurements, a total amount of $(1.75 \pm 0.3) \times 10^{-6}$ mole fraction of divalent impurities was found to be present in these samples.

A. Diffusion

Diffusion was carried out first by evaporating onto the "pure" NaI sample a thin layer (0.05–0.1μm) of NaI containing copper impurity. This copper impurity source was obtained by heating small blocks of "pure" NaI crystal with a small piece of high-purity copper foil at a temperature of about 600°C for about three days in a helium atmosphere.

An alternative impurity source was to use CuI. Since CuI has a vapor pressure of about two orders of magnitude higher than NaI, it is more desirable to use NaI containing the impurity. The annealing of the evaporated samples which were set in a quartz tube was carried out in a helium atmosphere at atmospheric pressure or slightly below. Temperatures were measured with *Pt* and *Pt* + 10-wt% Rh thermocouples which were in actual contact or very close to the samples. The annealing times were determined so that $5(Dt)^{1/2} \lesssim 0.20$ cm, where D is the temperature-dependent diffusion coefficient and t is the annealing time. Corrections were necessary for the heating and cooling portions of the diffusion cycle if the annealing times were short (less than 1 h). To minimize the heating time, samples were pushed into the furnace by the thermocouples while the quartz tube envelope was maintained at equilibrium temperatures with the furnace. In this way, samples were within 1°C of diffusing temperature in 100 sec.

With the above experimental boundary conditions, the solution of Fick's second law for the semi-infinite system is

$$C(z, t) = \frac{S}{(\pi D t)^{1/2}} e^{-z^2/4Dt}, \qquad (2.1)$$

where S is the total diffusing substance per unit area initially deposited on the surface. This solution assumes that the diffusion coefficient D is a constant. A plot of $\log_{10} C$ vs z^2 (z is the penetration depth) then gives a straight line for a given set of experimental data. Deviation from a straight line (beyond experimental error) means that D is not a constant and is concentration dependent.

B. Determination of copper concentration

An optical-absorption method was used to determine copper concentrations in NaI. Theoretically, the concentration of a given impurity center is proportional to the product of its absorption band width and its absorption coefficient.[17–19] For the case of copper centers in NaI, we have found that the half width, which is equal to 0.26 ± 0.005 eV at -190°C is a constant at dilute concentrations, so that the concentration is actually proportional to the absorption coefficient at the peak of the copper absorption band ($\lambda = 256.3$ nm). Bateman and Van Sciver[20] have determined the copper absorption coefficient μ in NaI as a function of its concentration C: $\mu/C = (2.0 \pm 0.2) \times 10^{+6}$ cm^{-1}, where C is in mole fraction. This equation applies for $0 < C \lesssim 20$ ppm. In order to avoid the introduction of errors because of luminescent emission from copper centers as well as exciton (intrinsic) luminescence, the maximum concentration for final analysis was kept below 13 ppm (with a few exceptions).

All optical absorption measurements were carried out at -190 ± 0.5°C.

C. Determination of penetration depth

The method is a refinement of that introduced by Reisfeld *et al.*[21] In our case, a Bausch and Lomb double grating monochromator is used to illuminate a 30-μm slit behind which the crystal sample may be moved by means of a micrometer (Fig. 1). The crystal faces through which measuring light passes were freshly cleaved before crystal placement in the measuring apparatus. The mount is provided with masks which restrict the effective length of the illuminating slit. Crystal layers larger than $5(Dt)^{1/2}$ were either cleaved away or blocked out from the optical path. Thus, any copper which might diffuse inward from the sides of the sample and be detected by its absorption was negligible.

For the critical purpose of locating the initial high-concentration surface (the edge of the crystals), two identical samples cleaved from the same diffused block were mounted on the sample holder end to end with the high-concentration surfaces making contact. Samples were cleaved in a special cleaving device so that all the high-concentration edges would remain near perfectly parallel and sharp. An axis of symmetry could thus be determined after the concentration-distance curve had been plotted. This located crystal edges to within 5 μm. (Two sets of plots of $\log_{10} C$ vs z^2 allowed us to make an adjustment of the symmetric axis, if necessary.)

III. RESULTS AND DISCUSSION

A. Results

Figure 2 shows a typical penetration profile obtained from an initial thin-layer boundary. Usually, data points within 0.15 mm of the symmetric axis are unreliable because of reflection and diffraction near the edges. Additional light passing through the small gap of the contact edges sometimes is significant.

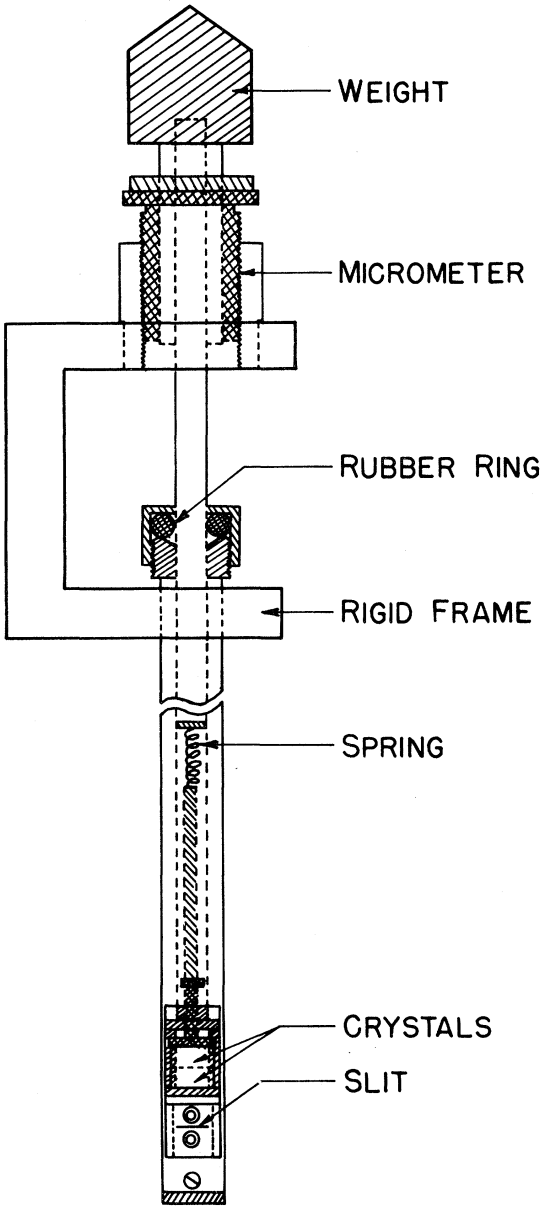

FIG. 1. Sample holder for optical-absorption measurement.

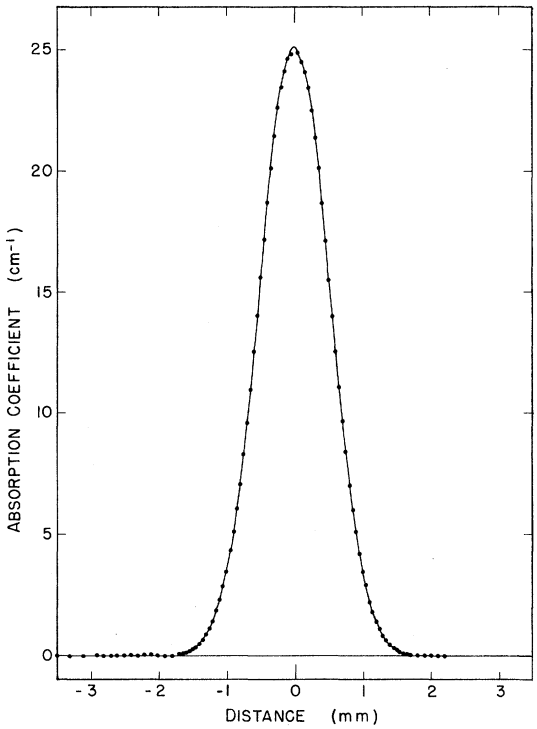

FIG. 2. Penetration profiles of copper diffusion in NaI.

Figures 3–5 show the penetration profiles plotted as $\log_{10}C$ vs z^2. Here C's are represented by their corresponding absorption coefficients. These curves have been shifted up or down arbitrarily. Some of the curves (3.3, 3.4, 4.1, 5.1) bend downwards near the top because luminescent light from copper centers becomes significant in comparison with the transmitted light when the absorption coefficient is high. The "apparent" absorption coefficient calculated would be smaller than the actual copper absorption coefficient. However, this difficulty does not affect the accuracy of the diffusion coefficients to be determined from the slopes.

It is important to observe that the plots of $\log_{10}C$ vs z^2 are linear only at temperatures below 265°C and above 415°C, and they are curved upwards at temperatures inbetween. The curvature increases gradually as the temperature increases from 265°C and it starts decreasing as the temperature goes beyond about 350°C. Furthermore, the Arrhenius plot (Fig. 6) of those diffusion coefficients obtained from the constant slopes shows two distinct straight segments with the break in slopes occuring within the temperature region where the penetration profiles are non-Gaussian. From the two slopes, activation energies are calculated to be $E_2 = 1.00 \pm 0.01$ eV for the low-tem-

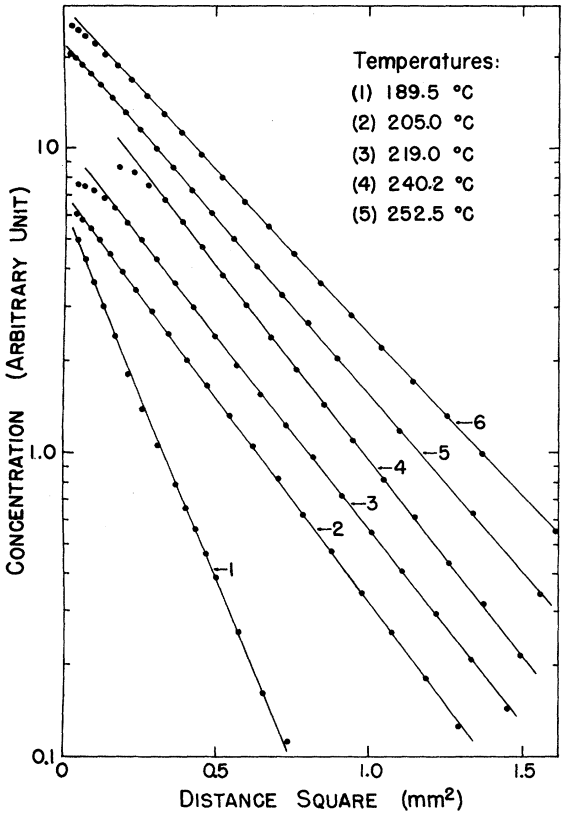

FIG. 3. Plots of $\log_{10}C$ vs z^2 at various temperatures.

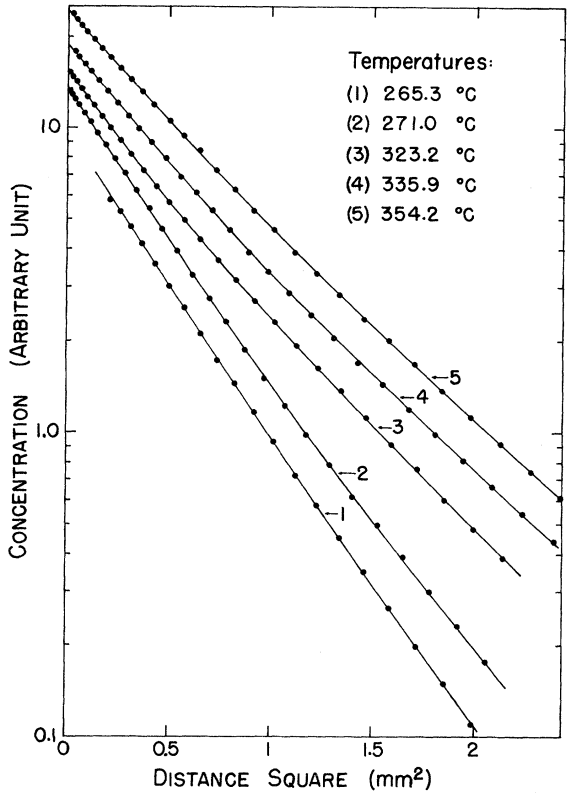

FIG. 4. Plots of $\log_{10}C$ vs z^2 at various temperatures.

perature region (below 265 °C) and $E_1 = 0.65 \pm 0.005$ eV for the high-temperature region (above 415 °C). Incidentally, these two temperature regions fall into the extrinsic- and the intrinsic-temperature regions, respectively, for the samples which we used. Most of the calculated data are collected in Table I. Many other data which are not presented here are consistent with the above description.

B. Diffusion model

This special diffusion behavior has not been observed in any alkali halide although copper[1] diffusion in AgCl and AgBr and gold[2] in AgCl behave similarly in most respects. There are three major distinctions in which the diffusion of copper in NaI differs from other monovalent impurity diffusion in the alkali halides reported. First, $E_2 > E_1$ and $E_1 < \frac{1}{2}h_s$ (where h_s is the enthalpy of formation of Schöttky defects, and h_s is given to be[22] 2.27 eV for NaI); second, the impurity diffusion coefficient exceeds the self-diffusion coefficient over three orders of magnitude (Fig. 7) within the temperature region of investigation; and third, a non-Gaussian penetration region sandwiches between two Gaussian penetration regions. The first distinction strongly suggests that copper cannot migrate via a simple vacancy mechanism at high temperature since this would require $E_1 = \frac{1}{2}h_s + h_m + h_b - k[\partial \ln f/\partial(1/T)]$, where h_b is the impurity-vacancy binding energy and f is the correlation factor for impurity diffusion. The last three terms are unlikely to give a combined value of -0.58 eV for each of them is of the order of a few tenths of an eV. In fact, copper is unlikely to migrate via a simple vacancy mechanism at low temperature either, for if copper diffuses by the same (vacancy) mechanism as sodium, the ratio of the diffusion coefficients ususally would not exceed an order of magnitude. Both would be limited by the amount of vacancies available.

The special structure of the Arrhenius plot (Fig. 6) and the non-Gaussian penetration profiles in the intermediate-temperature region, require that there must be two mechanisms (other than vacancy) participating in the transport of copper in NaI. One mechanism is responsible (or domin-

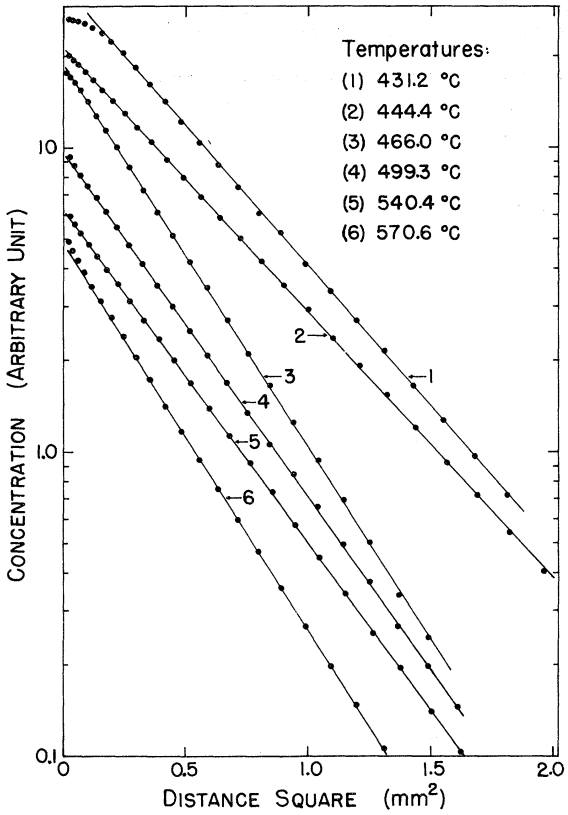

FIG. 5. Plots of $\log_{10}C$ vs z^2 at various temperatures.

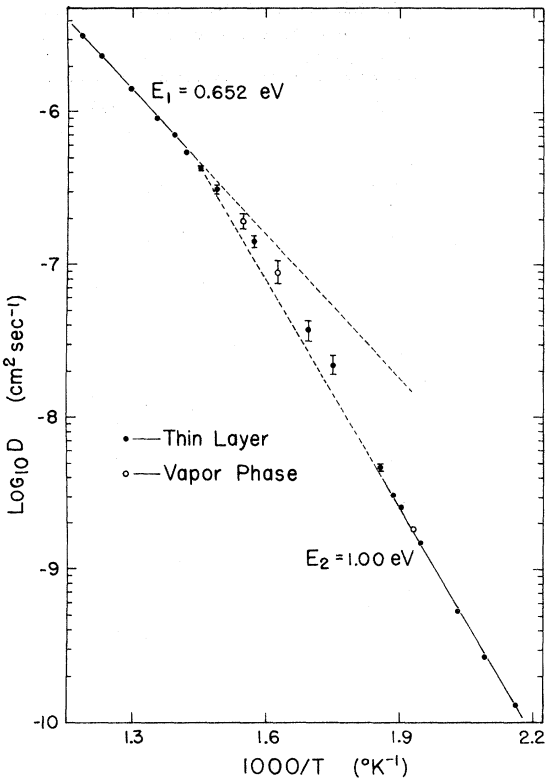

FIG. 6. Arrhenius plot of copper impurity diffusion coefficient in NaI.

ant) for migration of copper in each of the extreme-temperature regions, and each mechanism is practically independent of copper concentration in its respective temperature range (since the penetration profiles are Gaussian). For the intermediate-temperature region, both mechanisms are involved. The proportion that each mechanism carries is a function of concentration and temperature. To be more specific, it is governed by the mass-action relations inside the crystal. Hence, if the diffusion rates of the two mechanisms are not equal, their apparent or effective diffusion coefficient will vary according to the changes of their proportions. Thus, it is understandable that all plots of $\log_{10}C$ vs z^2 in the temperature region between 265 and 415°C are curved, since the solution of the simple Fick's equation (constant D) is no longer applicable here. The transitions from one-mechanism domination to a two-mechanism coexistence and from a two-mechanism coexistence to another mechanism domination are gradual and smooth as is obvious from the changes of curvatures of $\log_{10}C$-vs-z^2 plots. Therefore, the boundary between any two temperature regions cannot be defined clearly. The temperatures 265 and 415°C are chosen only for convenience.

Since a simple vacancy mechanism is not involved in the transport of copper in NaI, the choice of the two proposed diffusion mechanisms is rather narrow. With a small activation energy (0.65 eV) obtained from the high-temperature Arrhenius plot, an assignment of interstitial mechanism for the high-temperature copper diffusion seems to be fairly reasonable. Süptitz[1] and Batra *et al.*[2] also proposed an interstitial mechanism for the diffusion of copper in AgCl and AgBr and gold in AgCl at high temperature. Direct evidence of an interstitial mechanism for copper in NaI will be given in Sec. III C. The diffusion mechanism for the low-temperature range (190–265°C), however, is currently unknown. Copper has been known to occupy lattice sites at low temperature[23,24] and has a tendency to sit off-center[24] in the [111] direction in alkali halides. Therefore, the low-temperature mechanism might involve complex pairs of an interstitial copper ion and a cation vacancy.

TABLE I. Diffusion coefficients of copper in NaI single crystal at various temperatures. The pre-exponential factors D_0 and the activation energies E are obtained for the two temperature regions.

T(°C)	D(cm^2/sec)	D_0(cm^2/sec)	E(eV)
189.5	1.320×10^{-10}		
205.0	2.686×10^{-10}		
219.0	5.375×10^{-10}	10.0 ± 1.3	1.00 ± 0.01
240.2	1.542×10^{-9}		
252.5	2.646×10^{-9}		
256.8	3.085×10^{-9}		
265.3	(4.65×10^{-9}) [a]		
271.0	curved		
281.1	curved		
297.8	(2.19×10^{-8})		
304.1	curved		
316.6	(3.74×10^{-8})		
323.2	curved		
335.9	curved		
342.8	curved		
354.2	curved		
363.0	(1.43×10^{-7})		
380.0	curved		
397.8	(3.17×10^{-7})		
414.8	(4.31×10^{-7})		
431.2	5.460×10^{-7}		
444.4	6.720×10^{-7}		
466.0	9.060×10^{-7}	$(2.6\pm0.02)\times10^{-2}$	0.652 ± 0.005
499.3	1.420×10^{-6}		
540.4	2.330×10^{-6}		
570.6	3.200×10^{-6}		

[a] Numbers in parentheses are obtained either from the straight segments or the averaged slopes of the plots of $\log_{10}C$ vs z^2.

C. Evidence of interstitial mechanism

Unlike a divalent impurity ion, a monovalent copper ion that enters substitutionally in NaI does not create an extra vacancy. However, if the copper ion enters interstitially, a vacancy will be created to conserve charge. With this idea in mind, it was suggested[25] to us that measurements of ionic conductivity on both "pure" and copper-doped samples should give a strong indication whether copper ions did indeed go into interstitial positions. The results of those measurements are shown in Fig. 8. The behavior of the curve labeled "copper doped" shows a very different structure than the familiar divalent impurity-controlled conductivity plots. Therefore, the increment of conductivity cannot be due to accidental contamination by divalent impurities during sample preparation. It is also suggested that copper cannot be in its divalent state. The smaller conductivity near the low-temperature region is believed due to suppression of vacancies by sodium (or copper), since the sample was prepared by heating with a piece of pure-copper foil. At any rate, the increment of ionic conductivity observed is consistent with the incorporation of interstitial ions. Besides this, there is no other way, within the present defect models available, to explain such an increment.

IV. THEORY AND QUANTITATIVE ANALYSIS

A. Theory

The chemical reactions which occur inside the NaI:Cu system are

$$L_{Cu} \rightleftarrows I^+_{Cu} + V^-_{Na} \quad \text{(Frenkel)}, \tag{4.1}$$

$$0 \rightleftarrows V^-_{Na} + V^+_{I} \quad \text{(Schöttky)}, \tag{4.2}$$

where L_{Cu} refers to a lattice-site copper ion, I^+_{Cu} refers to an interstitial copper ion, V^-_{Na} is cation vacancy, and V^+_I is anion vacancy. Under equilibrium conditions, these reactions have to obey the mass-action laws.

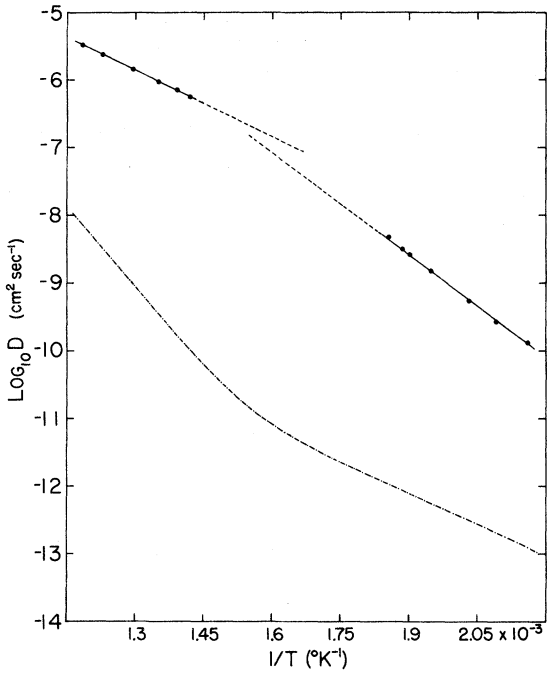

FIG. 7. Arrhenius plots of D_{Na} and D_{Cu} in NaI. D_{Na} are obtained from Hoodless's data (Ref. 22) and our conductivity data in the extrinsic temperature region.

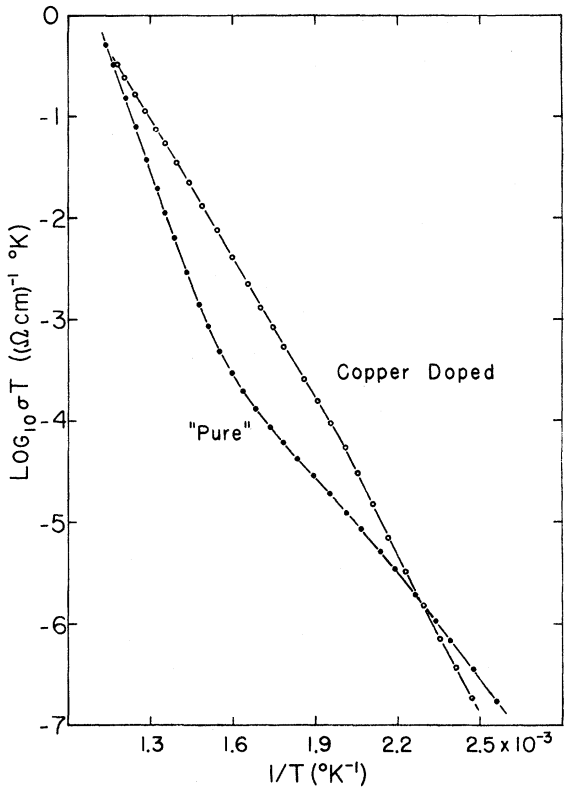

FIG. 8. Plot of σT vs reciprocal absolute temperature of "pure" NaI and copper-doped NaI.

$$x_0 x_{Na} = K_f x_g \,, \tag{4.3}$$

$$x_{Na} x_I = K_s \,, \tag{4.4}$$

where x_0, x_g, x_{Na}, and x_I are concentrations of interstitial copper ions, substitutional copper ions, cation vacancies, and anion vacancies, respectively. Each of these mobile defects obeys a continuity equation of the form

$$\partial x_i/\partial t + \operatorname{div} \vec{J}_i = (\partial x_i/\partial t)_{\text{reaction}} \,, \tag{4.5}$$

where x_i is the concentration of the ith species, J_i is the current density, and the right-hand side expression is the formation rate of the ith species due to chemical reaction. Generally, each current density J_i consists of two terms

$$J_i = -D_i \,\partial x_i/\partial z \pm \mu_i x_i \,\partial\varphi/\partial z \,, \tag{4.6}$$

where D_i is the diffusion coefficient, μ_i is the mobility, and $-\partial\varphi/\partial z$ is the electric field. However, if no external field is applied and the assumption of charge neutrality is valid everywhere throughout the diffusing process, the $\partial\varphi/\partial z$ term will be equal to zero. There was no evidence that the diffusion-penetration profiles varied with time besides normal penetration. Further, these profiles were Gaussian and the diffusion coefficients were time independent in the extreme-temperature regions. This indicates that the assumption in our system is a reasonable one. Hence, the continuity equation for x_0 and x_g are

$$\frac{\partial x_0}{\partial t} - \frac{\partial}{\partial z}\left(D_0 \frac{\partial x_0}{\partial z}\right) = \left(\frac{\partial x_0}{\partial t}\right)_{\text{reaction}} \,, \tag{4.7}$$

$$\frac{\partial x_g}{\partial t} - \frac{\partial}{\partial z}\left(D_g \frac{\partial x_g}{\partial z}\right) = -\left(\frac{\partial x_0}{\partial t}\right)_{\text{reaction}} \,, \tag{4.8}$$

since $(\partial x_g/\partial t)_{\text{reaction}} = -(\partial x_0/\partial t)_{\text{reaction}}$. Eliminating $(\partial x_0/\partial t)_{\text{reaction}}$ from Eqs. (4.7) and (4.8), one has

$$\frac{\partial x}{\partial t} = \frac{\partial}{\partial z}\left(D_0 \frac{\partial x_0}{\partial z} + D_g \frac{\partial x_g}{\partial z}\right)$$

or

$$\frac{\partial x}{\partial t} = \frac{\partial}{\partial z}\left(D_0 \frac{x_0'}{x'} + D_g \frac{x_g'}{x'}\right)\frac{\partial x}{\partial z} \,, \tag{4.9}$$

where x is defined to be $x = x_0 + x_g$, the total-copper concentration. Comparison of Eq. (4.9) with the diffusion equation $D(x)$ can be identified immediately

$$D(x) = D_0 \frac{x_0'}{x'} + D_g \frac{x_g'}{x'}$$

$$= D_g + (D_0 - D_g)\frac{x_0'}{x'} \,. \tag{4.10}$$

For charge neutrality, one has

$$x_{\mathrm{Na}} - x_{\mathrm{I}} - x_0 - x_d = 0, \tag{4.11}$$

where x_d is the concentration of free (dissociated) divalent impurity which obeys

$$x_{\mathrm{Na}} x_d = (x_p - x_d) K_d . \tag{4.12}$$

Here, x_p is the total divalent impurity concentration and K_d is the equilibrium constant involved. From Eqs. (4.3), (4.4), (4.11), and (4.12), one is able to show that

$$\frac{x_0'}{x'} = \frac{f(x_{\mathrm{Na}}, x_d)}{f(x_{\mathrm{Na}}, x_d) + x_0 x_g / x_{\mathrm{Na}} x} \frac{x_0}{x} , \tag{4.13}$$

where

$$f(x_{\mathrm{Na}}, x_d) = 1 + \frac{K_s}{x_{\mathrm{Na}}^2} + \frac{x_d(x_p - x_d)}{x_{\mathrm{Na}} x_p} . \tag{4.14}$$

B. Numerical solution

In order to apply a convenient constant-boundary condition at $z = 0$, a new function C is introduced such that

$$C = \int_z^\infty x \, dy , \tag{4.15}$$

and is satisfied by the diffusion equation

$$\partial C/\partial t = D(x) \partial^2 C/\partial z^2 . \tag{4.16}$$

An appropriate difference equation for Eq. (4.16) is given to be

$$\begin{aligned} \frac{(\delta^2 C)_j^{n+1} + (\delta^2 C)_j^n}{2(\Delta z)^2} = {} & \frac{A_{j+1}}{12} (C_{j+1}^{n+1} - C_{j+1}^n) \\ & + \frac{5A_j}{6} (C_j^{n+1} - C_j^n) \\ & + \frac{A_{j-1}}{12} (C_{j-1}^{n+1} - C_{j-1}^n) \\ & + O((\Delta t)^2) + O((\Delta z)^4) , \end{aligned} \tag{4.17}$$

where

$$(\delta^2 C)_j^n = C_{j+1}^n - 2C_j^n + C_{j-1}^n , \tag{4.18}$$

and

$$A_j = \frac{D_j^n + D_j^{n-1}}{2(D_j^n)^2 \Delta t} . \tag{4.19}$$

The space interval Δz is chosen to be 0.0025 cm in all the calculations. This requires J (total space intervals) to be about 140 so that $0 \approx C_j < 10^{-10} C_0$ is true at all times. As soon as Δz is fixed, a value of Δt such that $\Delta t \lesssim (\Delta z)^2/6D(x)_{\min}$ can be found. $D(x)_{\min}$ is the minimum diffusion coefficient calculated from Eq. (4.10) for a given set of values of the parameters given in Sec. IV A. These values of Δz and Δt have been tested against a set of values two times smaller for the same $D(x)$. It is found that the difference between the $C(z)$ profiles generated by those two sets of values is less than 0.01%.

In Sec. IV A one finds that $D(x)$ is a six-parameter function, namely, x_p, K_s, K_d, K_f', D_0, and D_g. For our samples, x_p (total-divalent-impurity concentration) is found to be 1.75 ppm. Comparison of our conductivity data with those of Hoodless[22] also gives a consistent value. K_s and K_d are calculated from ionic conductivity parameters such that

$$K_s = \exp(S_s/k - h_s/kT) , \tag{4.20}$$

$$K_d = \tfrac{1}{12} \exp(S_d/k - h_d/kT) , \tag{4.21}$$

where

$$S_s = (8.74 \pm 0.25)k ,$$

$$h_s = (1.97 \pm 0.02) \text{ eV} ,$$

$$S_d = (4.20 \pm 0.15)k ,$$

and

$$h_d = (0.51 \pm 0.03) \text{ eV} .$$

These ionic conductivity parameters are obtained from a least-squares fit of the conductivity data of the "pure" sample. The fitting procedure is solely based on cationic vacancy conduction. No systematic variation with temperature between the data points and the best-fit curve is observed. So, any correction (such as anionic vacancy conduction or Debye-Hückel corrections) to be incorporated is unlikely to be significant. With the fixed values of x_p, K_s, and K_d, there remains K_f, D_0, and D_g to be determined by seeking the best-fit profile for each of the experimental profiles. It might be worth pointing out that Hoodless's, *et al.* values of S_s and h_s have been found to be too large from the earlier calculations (S_d and h_d are in good agreement). With Hoodless's values of S_s and h_s, it is found that the values of K_f, D_0, and D_g obtained by fitting the generated theoretical profiles with the experimental profiles cannot be fitted into an exponential form. Most of the troubles are in the high-temperature region, since Hoodless's values of S_s and h_s give rather large values of K_s at high temperatures. This, in turn, results in nonexponential temperature dependence of K_f, D_0, and D_g. In fact, Hoodless's value of h_s has been indicated to be too large by other investigators.[27] Incidentally, the 1.97 eV obtained for h_s fits almost exactly in the equation,[26] $h_s = 2.14 \times 10^{-3} T_m$ (in eV). For these reasons, the above values of S_s and h_s are confidently accepted in our calculations.

Since a least-squares-fit calculation is not practical here, a step-by-step adjustment method is used instead. This method is aided greatly by the fact that D_0, D_g, and K_f are exponential functions of temperature since both diffusion and creation of copper defects in NaI are thermally activated processes. Because of this restriction, the adjustable ranges of the parameters will become smaller and smaller as the fitting of the experimental data has been extended to a wider temperature range. In the beginning, an additional set of data usually requires further adjustments of the "best-fit" parameters obtained previously. Such adjustments will be insignificant when the fitting has covered all the three temperature ranges. All of the theoretical curves are fitted to the experimental profiles everywhere within the first two decades to better than 5%. Actually, the first decade always fits better than 2%. The accuracy of K_f, D_0, and D_g resulted in best-fit curves is comparable to these values. Some trial calculations have indicated that a 20% error in x_p would give a 2% error in E_f, an activation energy calculated from the Arrhenius plot of K_f, and a value of h_s 5% larger (or 10% smaller) than 1.97 eV would result in difficulty of fitting.

C. Results and discussion

All of the theoretical parameters which resulted in "best-fit" curves are collected in Table II and plotted in Figs. 9 and 10. The shift of D_0 and D_g with respect to the actual experimental curves (lines) are clearly shown. This indicates that the contribution of one mechanism is not really negligible in comparison with the dominant one. The "minor" mechanism can contribute up to about 30% of total copper diffusion in each of the extreme-temperature regions. The activation energies $E_0 = 0.545 \pm 0.01$ eV and $E_g = 0.957 \pm 0.01$ eV obtained from the Arrhenius plots of D_0 and D_g are the true migration energies of interstitial and the "unknown" mechanisms, respectively. The activation energy $E_f = 1.085 \pm 0.02$ eV obtained from the plot of K_f is the formation energy of a copper-vacancy Frenkel pair in NaI. Experi-

TABLE II. Ionic parameters of copper impurity in sodium iodide obtained from theoretical analysis.

T (°C)	Time (sec)	D_0 (cm^2/sec)	D_g (cm^2/sec)	K_f mole fraction
189.5	3 370 560	5.30×10^{-9}	1.27×10^{-10}	1.63×10^{-9}
205.0	2 968 200	8.20×10^{-9}	2.51×10^{-10}	3.80×10^{-9}
219.0	1 585 800	1.18×10^{-8}	4.87×10^{-10}	7.80×10^{-9}
240.2	554 400	2.04×10^{-8}	1.23×10^{-9}	2.30×10^{-8}
252.5	354 960	2.78×10^{-8}	2.10×10^{-9}	4.16×10^{-8}
256.8	327 600	2.98×10^{-8}	2.37×10^{-9}	5.00×10^{-8}
265.3	250 620	3.65×10^{-8}	3.30×10^{-9}	7.00×10^{-8}
271.0	203 220	4.06×10^{-8}	4.11×10^{-9}	9.10×10^{-8}
281.1	118 800	5.10×10^{-8}	6.14×10^{-9}	1.43×10^{-7}
297.8	119 100	7.07×10^{-8}	1.015×10^{-8}	2.70×10^{-7}
316.6	58 560	9.85×10^{-8}	1.97×10^{-8}	5.45×10^{-7}
335.9	25 170	1.40×10^{-7}	3.67×10^{-8}	1.08×10^{-6}
342.8	15 960	1.565×10^{-7}	4.50×10^{-8}	1.38×10^{-6}
354.2	15 120	1.87×10^{-7}	6.33×10^{-8}	1.97×10^{-6}
363.0	10 500	2.16×10^{-7}	7.78×10^{-8}	2.56×10^{-6}
380.0	4440	2.91×10^{-7}	1.28×10^{-7}	4.50×10^{-6}
414.8	3660	4.75×10^{-7}	3.05×10^{-7}	1.20×10^{-5}
444.4	1800	6.90×10^{-7}	6.00×10^{-7}	2.56×10^{-5}
466.0	930	8.76×10^{-7}	9.06×10^{-7}	4.20×10^{-5}
499.3	660	1.26×10^{-6}	1.715×10^{-6}	8.73×10^{-5}
540.4	427	1.88×10^{-6}	3.54×10^{-6}	1.99×10^{-4}
570.6	265	2.48×10^{-6}	5.71×10^{-6}	3.48×10^{-4}
Activation energy (eV)		0.545 ± 0.01	0.957 ± 0.01	1.085 ± 0.02
Pre-exponential factor		$(4.5\pm1.2)\times10^{-3}$	3.1 ± 0.6	$(1\pm0.5)\times10^{3}$

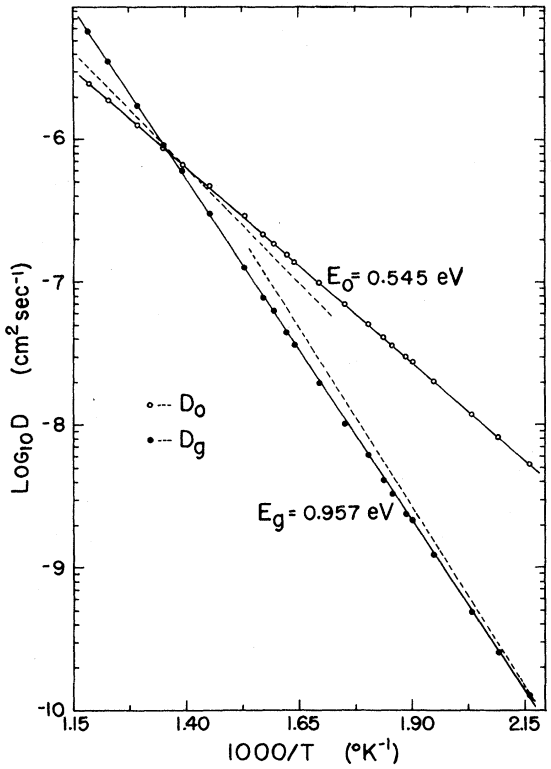

FIG. 9. Arrhenius plots of D_0 and D_g. The dash lines represent the actual experimental data plotted in Fig. 6.

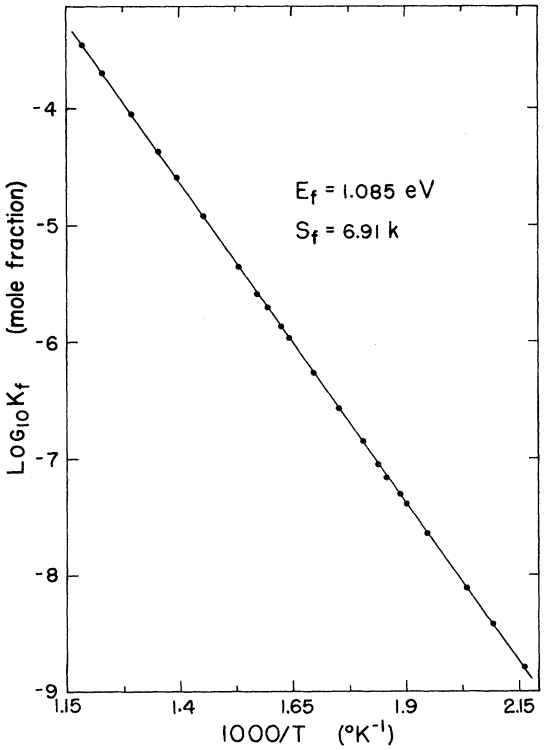

FIG. 10. Plot of K_f, the formation constant of interstitial copper ions in NaI.

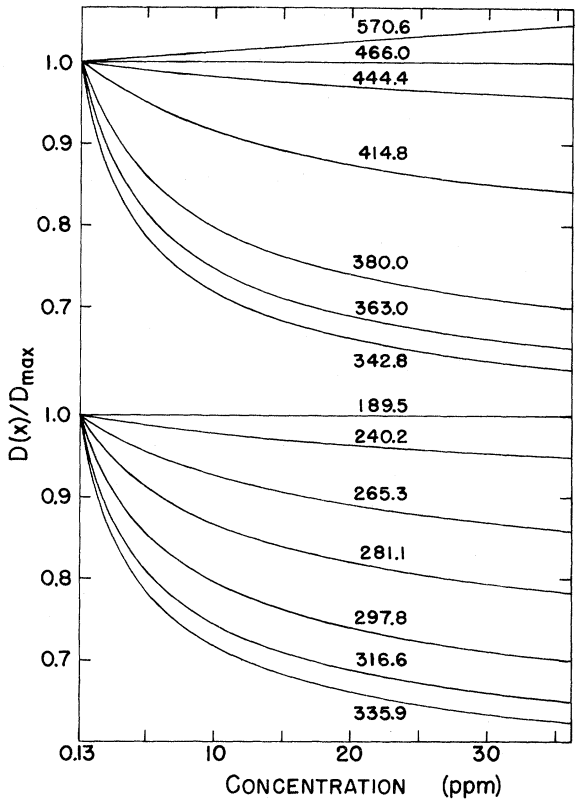

FIG. 11. Plots of $D(x)$ at various temperatures indicated in °C. Each of them is divided by D_{max}, its diffusion coefficient at $x = 0.13$ ppm.

mentally, it is found to be 0.94± 0.06 eV from the conductivity data of the copper-doped sample. From Fig. 10, an activation energy of 0.94± 0.03 eV, obtained from the high-temperature conductivity plot, is equal to $h_m + h_f/2$, where h_f is the enthalpy for the formation of a free Frenkel copper-vacancy pair. If $h_m = 0.47$[22] is used, h_f is calculated to be 0.94± 0.06 eV. The agreement of the theoretical and the experimental value is reasonably good. This small activation energy explains why the formation of Frenkel defects is favored over Schöttky defects.

In Fig. 11, 14 plots of $D(x)$, which produce the best-fit curves, are shown. Note that the maximum variation of $D(x)$ is at a temperature between 335.9 and 342.8°C where the plot of $\log_{10}C$ vs z^2 should give a maximum curvature. The curvature of the plots decreases as the temperature either increases or decreases. If the variation of $D(x)$ is less than 10% in the concentration range given in the figures, the curvature will be too small to be observable on an experimental plot, i.e., one can always put a straight line through the data points. In other words, a straight

line of the plot does not mean that D is truly a constant. A maximum variation of 10% should be allowed for the diffusion coefficient. At temperature higher than 465°C, $D(x)$ increases while concentration increases. A similar phenomenon is observed by Süptitz[28] for copper diffusion in AgBr. His results at other temperatures are comparable to ours except at high concentration where the theory is not applicable.

V. CONCLUSION

The diffusion study of copper in NaI has led to a further understanding of an extraordinary impurity center existing in an alkali halide. Its diffusional behavior in NaI is sufficiently different than that of the other impurity diffusion reported in the alkali halides that Frenkel disorder is proposed to be its predominant type defect. This is strongly supported by the conductivity measurements which show a tremendous increment of ionic conductivity by doping the sample with copper.

This special diffusion behavior also requires two mechanisms to govern the migration of copper in NaI. The high-temperature diffusion is dominated by an interstitial mechanism, while the low-temperature diffusion is dominated by an unknown mechanism. This unknown mechanism has to be a mechanism other than interstitial or vacancy.

A theory which is based on the two-mechanism model has successfully explained the diffusion profiles. The theoretical value of the formation energy of copper-vacancy Frenkel pair obtained from numerical analysis is in reasonable agreement with the experimental value obtained from conductivity measurements.

---

*Supported in part by NSF Grant No. GH-34518.

[1]P. Süptitz, Phys. Status Solidi 7, 653 (1964).
[2]A. P. Batra, A. L. Laskar, and L. Slifkin, J. Phys. Chem. Solids 30, 2053 (1969).
[3]E. W. Sawyer and A. L. Laskar, J. Phys. Chem. Solids 33, 1149 (1972).
[4]A. L. Laskar and L. Slifkin, Bull. Am. Phys. Soc. 11, 838 (1966); 15, 170 (1970).
[5]Y. Iida and Y. Tomona, J. Phys. Soc. Jpn. 19, 1264 (1964).
[6]R. Reisfeld and A. Honigbaum, J. Chem. Phys. 48, 5565 (1968).
[7]S. J. Rothman, L. N. Barr, A. H. Rowe, and P. G. Selwood, Philos. Mag. 14, 501 (1966).
[8]F. J. Keneshea and W. J. Fredericks, J. Phys. Chem. Solids 26, 501 (1965).
[9]P. Süptitz, Phys. Status Solidi 12, 555 (1965).
[10]V. B. Ptashnik and A. N. Naumov, Fiz. Tverd. Tela 12, 1496 (1970) [Sov. Phys.–Solid State 12, 1174 (1970)].
[11]A. L. Laskar, A. P. Batra, and L. Slifkin, J. Phys. Chem. Solids 30, 2061 (1969).
[12]G. Bre'bec and L. Slifkin, Commis. Energ. At. (Fr.) Report (1969) (unpublished).
[13]A. P. Batra, A. L. Laskar, G. Bre'bec, and L. Slifkin, Radiat. Eff. 4, 257 (1970).
[14]M. Chemla, C. R. Acad. Sci. (Paris) 238, 82 (1954).
[15]L. B. Harris, J. R. Hanscomb, and J. L. Schlederer, Phys. Lett. A 32, 163 (1970).
[16]K. Heneda, T. Ikeda, S. Yoshida, J. Phys. Soc. Jpn. 25, 643 (1968).
[17]W. B. Fowler, *Physics of Color Centers* (Academic, New York and London, 1968), p. 72.
[18]D. L. Dexter, Phys. Rev. 101, 48 (1956).
[19]A. Smakula, Z. Phys. 59, 603 (1930).
[20]R. L. Bateman and W. J. Van Sciver, Phys. Status Solidi (B) 46, 779 (1971).
[21]R. Reisfeld, A. Glasner, and A. Honigbaum, J. Chem. Phys. 42, 1892 (1965).
[22]I. M. Hoodless, J. H. Strange, and L. E. Wylde, J. Phys. C 4, 2737 (1971); 4, 2742 (1971).
[23]S. A. Mack and W. J. Van Sciver, Phys. Status Solidi (B) 46, 193 (1971).
[24]K. L. Yip and W. B. Fowler, Phys. Status Solidi (b) 53, 137 (1972).
[25]L. Slifkin (private communication).
[26]L. W. Barr and A. B. Lidiard, *Physical Chemistry* (Academic, New York, 1970), Vol. 10, Chap. 3.
[27]S. Chowdhury, S. K. Sen., and D. Roy, Phys. Status Solidi (B) 56, 403 (1973).
[28]P. Süptitz, Phys. Status Solidi 7, 667 (1964).